ENVIRONMENTAL RESEARCH
LETTERS

LETTER

Sea level rise projections up to 2150 in the northern Mediterranean coasts

A Vecchio[1,2,3,*], M Anzidei[3] and E Serpelloni[4]

[1] Radboud Radio Lab, Department of Astrophysics, Radboud University, Nijmegen, The Netherlands
[2] LESIA, Observatoire de Paris, Université PSL, CNRS, Sorbonne Université, Université de Paris, Meudon, France
[3] Istituto Nazionale di Geofisica e Vulcanologia, Rome, Italy
[4] Istituto Nazionale di Geofisica e Vulcanologia, Bologna, Italy
[*] Author to whom any correspondence should be addressed.

E-mail: a.vecchio@astro.ru.nl

Abstract

Vertical land movements (VLM) play a crucial role in affecting the sea level rise along the coasts. They need to be estimated and included in the analysis for more accurate Sea Level (SL) projections. Here we focus on the Mediterranean basin characterized by spatially variable rates of VLM that affect the future SL along the coasts. To estimate the VLM rates we used geodetic data from continuous global navigation satellite system stations with time series longer than 4.5 years in the 1996–2023 interval, belonging to Euro-Mediterranean networks and located within 5 km from the coast. Revised SL projections up to the year 2150 are provided at 265 points on a geographical grid and at the locations of 51 tide gauges of the Permanent Service for Mean Sea Level, by including the estimated VLM in the SL projections released by the Intergovernmental Panel on Climate Change (IPCC) in the AR6 Report. Results show that the IPCC projections underestimate future SL along the coasts of the Mediterranean Sea since the effects of tectonics and other local factors were not properly considered. Here we show that revised SL projections at 2100, when compared to the IPCC, show a maximum and minimum differences of 1094 ± 103 mm and -773 ± 106 mm, respectively, with an average value that exceeds by about 80 mm that of the IPCC in the reference Shared Socio-economic Pathways and different global warming levels. Finally, the projections indicate that about 19.000 km^2 of the considered Mediterranean coasts will be more exposed to risk of inundation for the next decades, leading to enhanced impacts on the environment, human activities and infrastructures, thus suggesting the need for concrete actions to support vulnerable populations to adapt to the expected SL rise and coastal hazards by the end of this century.

1. Introduction

Tide gauge measurements and satellite radar altimetry data show that the global mean sea level (GMSL) over the past two centuries is rising at faster rates with respect to the last millennia due to global warming (Vermeer and Rahmstorf 2009, Lambeck *et al* 2010, Church and White 2011, Kemp *et al* 2011, DeConto *et al* 2021, Palmer *et al* 2021). Changes in GMSL are due to the joint effect of thermosteric, barystatic, glacio-hydro-isostatic and land-hydrology components (Lambeck and Purcell 2005). The rate of rise of the GMSL was 1.7 [1.3–1.9] mm yr^{-1},

over the period 1901–2015, 3.7 [3.2–4.2] mm yr^{-1} over the period 2006–2018 and it will likely reach 5.2–12.1 mm yr^{-1} in the period 2080–2100, for the lowest and highest CO2 emission scenarios (Fox-Kemper *et al* 2021). Since at a given geographical location both the SL and the land surface are not static over time, the observed SL change along the coasts results from the combined action of solid Earth and oceanographic variations driven by geophysical and climate processes. At regional scale the SL can show large changes with respect to the GMSL due to the contributions of dynamic effects, glacial isostatic adjustment (GIA) and natural and anthropogenic

Vertical land movements (VLM) that depends on the geographical location (Lambeck *et al* 2010, Kopp *et al* 2014, Vecchio *et al* 2019, www.ipcc.ch). In particular, coastal subsidence and uplift due to tectonics and other natural or anthropogenic factors, act at rates up to several mm yr^{-1}. These effects can change the amplitude and impact of the SL rise by locally increasing or reducing its effects on the coastal areas (Lambeck *et al* 2011, Bucx *et al* 2015, Higgins 2016, Vousdoukas *et al* 2018, Oppenheimer *et al* 2019, Scardino *et al* 2020, 2022, Anzidei *et al* 2021, Jevrejeva *et al* 2023). Since the SL rise is a major factor of hazard in coastal regions where cultural, socio-economic and environmental losses are already occurring (Syvitski *et al* 2009, Strauss *et al* 2014, Kulp and Strauss 2019, Horton *et al* 2020, Tay *et al* 2022), understanding and including the VLM in the SL projections for the next decades become crucial for a more detailed estimation of the flooding hazard and socio-economic consequences in coastal areas.

The SL of the Mediterranean is rising since 1880 (Fenoglio-Marc *et al* 2012, 2013, Wöppelmann and Marcos 2012, Tsimplis *et al* 2013, Anzidei *et al* 2014, Meli *et al* 2023) affecting the low elevated coastal plains, river deltas and beaches with consequent coastal erosion and retreat and salinization of the water table, thus representing a significant factor of hazard for coastal populations and infrastructures (Antonioli *et al* 2017, Anzidei *et al* 2017, Nienhuis *et al* 2023). In addition, the Mediterranean region is the seat of historical cities (e.g. Venice, Istanbul, Alexandria among others), heritage sites and high-value environmental and industrial areas, all exposed to severe coastal hazard and flooding (Reiman *et al* 2018, Anzidei *et al* 2020, Strauss *et al* 2021, Scardino *et al* 2022). Detailed SL projections for the next decades in the Mediterranean are therefore needed for building up realistic marine flooding scenarios (Rizzo *et al* 2022 and references therein) and making people, stakeholders, and decision makers aware of the ongoing phenomenon for a conscious management of the coastal zone (Loizidou *et al* 2023).

The most updated projections released by the Intergovernmental Panel On Climate Change (IPCC) in the 6th Assessment Report (AR6, Fox-Kemper *et al* 2021) refer to global and regional sea levels and consider the contributions of several geophysical sources. In particular, the regional projections include the contribution of a long-term VLM extracted from the longest time series of sea level as obtained by selected tide gauges of the Permanent Service for mean Sea level (PSMSL, https://psmsl.org/). In this study we show and discuss the SL projections in the Mediterranean basin by revisiting the IPCC AR6 projections up to 2150 including the linear trend of the current rates of VLM as estimated from the analysis of ground displacement time series of continuous global navigation satellite system (GNSS) networks operating in the Euro-Mediterranean region. The sea level

projections in a gridded format at a resolution of 0.5° in latitude and longitude for the north Mediterranean basin and at the location of selected PSMSL stations, are provided to map the future variability of the SL along the coasts.

2. The Mediterranean basin

The Mediterranean region is the result of the evolution of the convergence between the African and Eurasian plates across an east-west boundary that has been active since the Late Cretaceous (Dewey *et al* 1973, Le Pichon *et al* 1988, Jolivet and Faccenna 2000, Faccenna *et al* 2014). These plates are still colliding at a velocity of a few millimetres per year as indicated by geodetic data (Devoti *et al* 2017, Serpelloni *et al* 2022). The seismicity of the region is characterized by well-defined seismic belts underlining the boundaries of minor plates and a complex pattern of crustal deformations (Jackson and McKenzie 1988, Rebai *et al* 1992, Vannucci and Gasperini 2004, Serpelloni *et al* 2007, 2022) that include active and quiescent volcanoes (volcano.si.edu). The present-time kinematics of the Mediterranean basin is characterized by several active tectonic structures in the region The present-time kinematics of the Mediterranean basin is characterized by several active tectonic structures in the region (Faccenna *et al* 2014). Among these, the Hellenic Arc system in the eastern Mediterranean, the subduction of the Calabrian Arc and the volcanic arc of the Aeolian Islands in the central Mediterranean are the most relevant. In this complex tectonic framework, geological and geodynamic processes are causing continuous and episodic earthquake-related crustal deformations that also affect the coastal areas (Ferranti *et al* 2010, Anzidei *et al* 2014).

The Mediterranean region has also experienced large sea level changes driven by the growth and decay of the large ice sheets culminating in the Last Glacial Maximum about 20.000 years ago. This results in the associated isostatic effect as the Earth′s gravity, shape and rotation respond to the changing surface loads of ice and water (Peltier 2001, Lambeck and Purcell 2005, Spada 2017). Direct information about current trends of VLM in the Mediterranean regions can be inferred from instrumental data through seismic strain analysis of focal mechanisms for about the last 140 Direct information about current trends of VLM in the Mediterranean regions can be inferred from instrumental data through seismic strain analysis of focal mechanisms for about the last 140 years and crustal deformation analysis based on continuous GNSS stations (Anzidei *et al* 2014).

3. VLM from GNSS data

The Mediterranean region is characterized by spatially variable horizontal and vertical crustal deformations, with large deviations in volcanic areas.
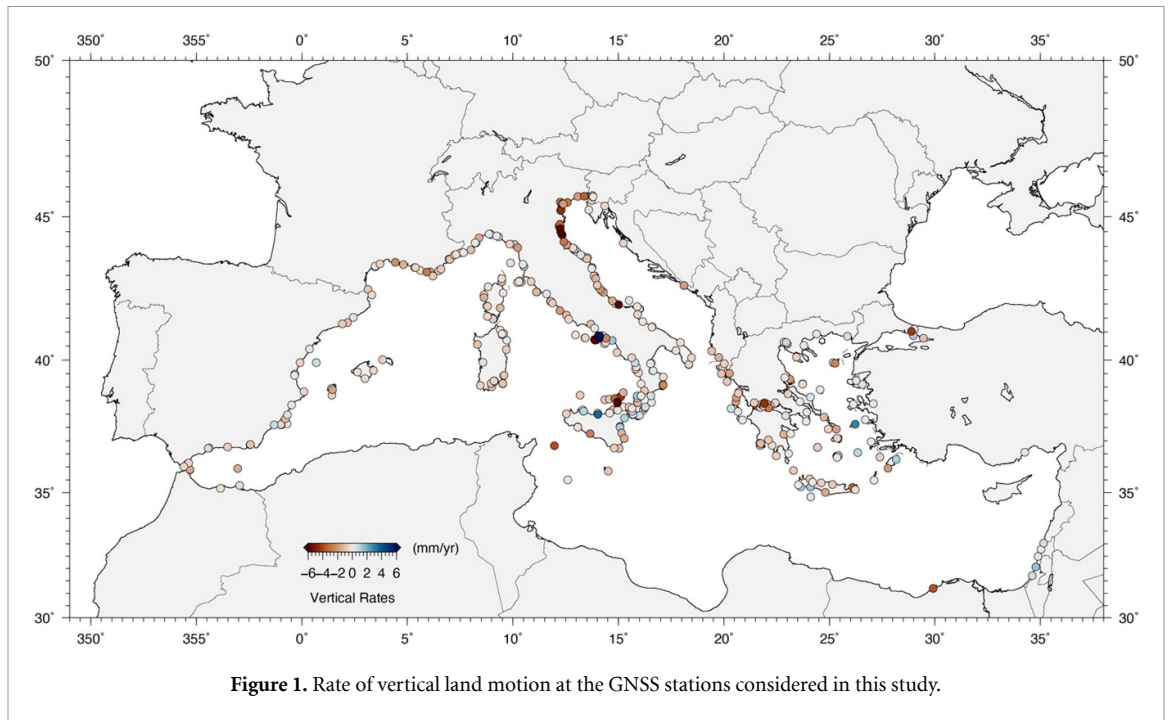
Figure 1. Rate of vertical land motion at the GNSS stations considered in this study.

To evaluate the impact of VLM on the SL, the vertical component of the crustal velocity field along the coasts of the Mediterranean region has been estimated by the analysis of the geodetic signal recorded at GNSS networks, managed by different institutions, in the Euro-Mediterranean and African areas (Esposito *et al* 2015, Devoti *et al* 2017, Marino *et al* 2022, Serpelloni *et al* 2022). Since we focus on the effects of VLM on the SL changes along the coasts, only GNSS stations located within 5 km from the coastline have been selected. Among these, to get a stable estimate of the vertical geodetic velocities, only time series longer than 4.5 years in the time interval 1996–2023 have been considered. This choice agrees with results from synthetic data suggesting that time series longer than 4.5 years are needed to get velocity accuracy of the order of mm yr^{-1} (Masson *et al* 2019). Analysis of GNSS data in the Euro-Mediterranean region shows that a median length of 6–7 years, with standard error ± 2.5 years, provides velocity estimates consistent with the ones obtained from longer time series (>10 years) (Serpelloni *et al* 2022). When the lower bound (4.5 years) is considered, velocity estimates are still consistent with results from synthetic data. The choice of 4.5 years cutoff value has thus been driven by the studies mentioned above and by the need to have a sufficiently large number of stations for the following analysis. In the same way the choice of a threshold distance of 5 km represents a good compromise between having a sufficiently large number of stations close to and a reasonable distance from the coast. This selection resulted in 638 GNSS stations (figure 1). Unfortunately, the geographical distribution of the selected stations is

not homogeneous since their number and density are higher in the North Mediterranean while only a few of them are operational in North Africa (at least concerning public available data), leading to only a partial picture of the current crustal motion across the Mediterranean region. Nevertheless, the spatial variability of the measured velocities highlights the different tectonic and volcanic environments of the Mediterranean region characterized by variable rates of VLM that can affect the SL change along the coasts.

GNSS velocities and uncertainties at the coastal stations have been obtained following the approach described in Serpelloni *et al* (2022), that includes: (i) the GNSS phase data reduction by GAMIT software (Herring *et al* 2010), (ii) by the GLOBK software and (iii) the time-series analysis. The reference frame has been obtained by minimizing coordinates and velocities of the IGS global core stations, while estimating a seven-parameter transformation with respect to the IGS realization of the ITRF2014 reference frame (Altamimi *et al* 2011). A maximum likelihood estimation method (Bos *et al* 2013) has been used to evaluate the stochastic noise content in the time series. Measured vertical velocities are in the range −17 (in the northern Adriatic) +36 mm yr^{-1} (in the Phlegrean fields). The uncertainties on the velocity estimates have been calculated using a white and a flicker noise model (Serpelloni *et al* 2022), which are suitable for the GNSS data in the Mediterranean region (Santamaría-Gómez *et al* 2011, Nguyen *et al* 2016). In figure 1 of the supplementary material a map of the vertical velocity uncertainties at each GNSS station is shown. Larger uncertainties are associated to noisier or shorter data. However,

since the uncertainty decreases the more the length exceeds 2.5 years (Serpelloni *et al* 2022), only a limited number of stations show uncertainties higher than 1 mm yr^{-1}. The mean uncertainty is 0.65 mm yr^{-1}.

In the Mediterranean area, the VLM pattern reflects the ongoing tectonic and non-tectonic processes. For example, the Venice lagoon (Italy) is undergoing land subsidence due to the combined effects of GIA, sedimentary, tectonic, and anthropogenic processes that locally accelerate the SLR. Conversely, along the sedimentary coast of Levant (Israel) and in the volcanic area of Phlegrean fields (Italy), the current uplift is slowing down the SLR.

4. Sea level projections

To evaluate the effect of the VLM on future sea levels, we considered the regional sea level projections provided in the 6th Assessment Report of the IPCC (Kopp *et al* 2023, Fox-Kemper *et al* 2021, Garner *at al* 2021), spanning the interval 2020–2150 (https://zenodo.org/record/6382554). In this work we used the medium confidence data that include only processes for which there is a general agreement in the scientific community (see e.g. Fox-Kemper *et al* 2021 for a detailed definition). AR6 projections are provided on both a $1° \times 1°$ worldwide grid and at the location of several tide gauges of the PSMSL network. AR6 projections are obtained by combining the contributions of several geophysical sources: the Antarctic Ice Sheet, the Greenland Ice Sheet (GIS), glaciers, land water storage, ocean dynamics (including thermal expansion) and VLM. For each gridpoint and PSMSL station, the quantile functions (107 quantiles from 0 to 1 in 0.01 increments) are available for the distribution of the total sea level change levels and rates and for each single contribution. The methods for deriving the sea level changes as a function of the quantiles and geographical location are not straightforward and can be different for each individual contribution. For example, to derive the contribution of the GIS, different SL projections are produced, by computing the probability distributions for two different ice sheet models and combined in a 'probability box' which represents the upper and lower bounds of the distribution. These methods are described in detail in the IPCC AR6 report (Fox-Kemper *et al* 2021).

The data are provided for all the scenarios considered in the AR6, namely the Shared Socioeconomic Pathways (SSP1-1.9, SSP1-2.6, SSP2-4.5, SSP3-7.0, SSP5-8.5) and the five global warming levels (Tlim: 1.5°, 2°, 3°, 4° and 5°C, higher than the current mean global temperature). Unlike the former IPCC projections, which included only the component of VLM associated with the GIA, the AR6 projections include a constant long-term background rate of change. The latter, including both the GIA and other

long-term VLM contributions, is extrapolated from historical tide gauge data to global coverage using a spatiotemporal statistical approach (Kopp *et al* 2014) and assumed to be the same for each scenario and constant over the considered time span. However, this approach can lead to an underestimation of the VLM in areas not yet monitored by tide gauge stations (Keogh and Törnqvist 2019) that can be affected by significant rates of land subsidence or uplift (e.g. due to fluid extraction, soil compaction, tectonics, or volcanism) (Minderhoud *et al* 2017).

To obtain more accurate SL projections in the Mediterranean area the AR6 projections have been revisited by including the trend of the VLM derived from the ground velocities from GNSS data. We assume that the VLM is linear, namely it will progress up to 2150 with the same rate as today. This assumption is reasonable, over a time scale of centuries, for the signal due to the regional secular tectonics (GIA and plate tectonics) (see e.g. Kato 1983, Bird *et al* 2009, Santamaría-Gómez and Mémin 2015, Palin *et al* 2020). Moreover, since the recurrence times of strong magnitude earthquakes ($M > 5.5$) in the Mediterranean area, producing vertical deformations on the coast capable of deviating the secular trend of the tectonic signal, is estimated to be hundreds or thousands of years (see e.g. DISS Working Group, 2021, and reference therein), we assumed that the VLM rate is not significantly affected over the time range considered for the revised SL projections (130 years). Unfortunately, it is not possible to define a recurrence time for volcanic events. In volcanic areas (as for example the Phlegraean Fields), the approximation of linear VLM trend depends on the dynamics of the volcanic structure that can produce local VLMs with time varying direction and rate. Despite these limitations, the assumption we made in this study is the most reasonable one, namely the current VLM directions and rates will remain constant over the time span of the SL predictions. We remark that in the IPCC AR6 report a similar linear approximation for the VLM is made worldwide thus suffering for the same uncertainties in volcanic areas.

The revised SL projections are calculated by adding the measured VLM to the median values of the AR6 IPCC projections data which do not include the VLM contribution (file ar6-regional_novlm-confidence.zip). The uncertainties on the revised projections are evaluated at each grid box as the sum of the squared uncertainties from the AR6 IPCC projections without VLM (as the distribution spread estimated from the 32nd and 68th percentiles) and the squared error from the GNSS velocity measurements. The choice of 4.5 years as minimum threshold for the GNSS time series does not affect the sensitivity of the VLM estimates with respect to the tide gauge estimates used by IPCC. The comparison of GNSS and IPCC based rates, as a function of the GNSS

series length (see supplementary material), shows no reduction in sensitivity for time series shorter than 6–7 years. At the same time no difference in sensitivity between tectonically active and volcanic areas is found.

5. Results and discussion

By analogy to the original IPCC AR6 data, the revised sea level projections in the range 2020–2150, are computed at different geographical locations:

1. Sea levels are evaluated at each PSMSL tide gauge location by considering the VLM rate from the closest GNSS stations (figure 2 panel (b)).
2. After rescaling the IPCC data to a $0.5° \times 0.5°$ grid, the VLM contribution in each cell is obtained as the median of the VLM rates from the GNSS stations falling into the cell (figure 2 panel (a)). If the cell does not encompass any GNSS station, the corresponding sea level projection is not calculated.
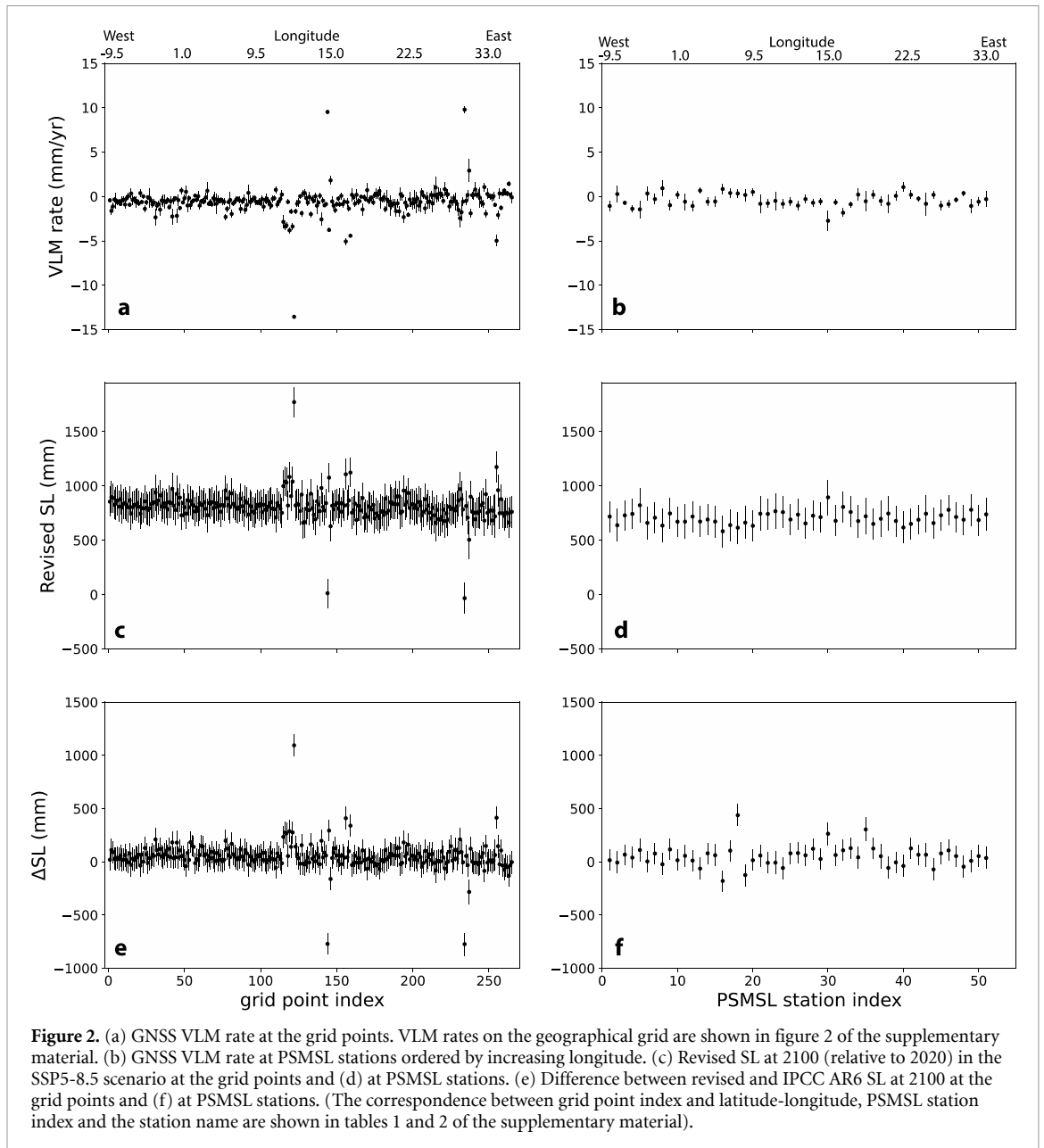
The revised SL at 2100 (relative to 2020) in the SSP5-8.5 scenario for each grid point and at the PSMSL stations are shown in panels (c) and (d) of figure 2. Examples of the sea level projections at four PSMSL tide gauges and at the four grid points encompassing them are shown in figures 3 and 4 for three SSP (namely 1-2.6, 3-7.0 and 8-8.5) and three global warming Tlim scenarios (namely 1.5°, 3°, 5°), respectively. The sea levels in 2050, 2100 and 2150 (relative to 2020) for all the considered IPCC scenarios are shown in tables 3 and 4 of the supplementary material. A comparison between the VLM contribution as provided by IPCC and from GNSS data, at the same PSMSL stations and grid points of figures 3 and 4, is shown in figure 5. The four chosen locations represent an example of sites where high rate of land subsidence (Venice and Po Delta/Marseille), and uplift (Hadera/Galilee coast and Phlegraean fields) are observed. For gridded data the comparison between revised and original IPCC AR6 SL projections (the latter are shown in figure 3 of the supplementary material) show significant differences (ΔSL) at 2100 varying between 1094 $\pm$103 mm and -773 ± 106 mm with an average value of 49 ± 6 mm (see figure 2 panel (e)). In the examples of figures 3 and 4, ΔSL at 2100/2150 varies between $-0.77/-1.2$ m for the Phlegraean fields to more than 1.1/1.8 m for the Po Delta. Values of ΔSL for the PSMSL stations are shown in figure 2 panel (f). ΔSL ranges between 438 ± 103 mm and -180 ± 100 mm at 2100 with an average value of 49 ± 6 mm. In the examples of figures 3 and 4, the VLM, although with slightly different values, shows the same sign of the trend for the stations of Venezia

Punta della Salute and Napoli Mandracchio while the measured VLM rate is opposite to the IPCC one at Hadera and Marseille (figure 5, panels (c) and (e)).

The observed differences between SL calculated on the grid and at PSMSL stations mainly arise from the different approach used to estimate the VLM trend, that is the median over a cell and the measurement at a given GNSS station. This difference is particularly remarkable in the north Adriatic coast of Venezia/Po delta (figures 3 and 4 panels (a)–(b)) and in the central Tyrrhenian coast of the Napoli/Phlegrean fields (figures 3 and 4 panels (g)–(h)) where the measured VLM rates are $-1.08 \pm 0.60/-13.6 \pm 0.2$ and $0.34 \pm 0.79/9.5 \pm 0.2$, respectively. The geological setting of both these areas is different and quite complex. The first is characterized by a general subsidence due to tectonics, soil compaction and ground fluid extraction, with a patchy VLM pattern with rates varying from -18.15 ± 0.19 to -2.78 ± 0.06. Spatially varying VLM is also found in the grid cell encompassing the Phlegrean fields area, characterized by active volcanic activity, where rates range between -0.43 ± 0.26 and 36.6 ± 1.0. The high variability of the VLM rate together with the high density of GNSS stations in this area cause the noticeable differences between the VLM calculated as the median value over a cell and the measurement at a single GNSS station thus resulting in significant differences in the corresponding SL projections. In the Phlegrean fields the area affected by volcanic deformation is very limited with an extension less than about 4 km^2. This implies that calculating the VLM rate as the median values of all the GNSS measurements falling into the cell, whose size is about 55×42 km^2, also stations that are not located in the volcanic area contribute to the median VLM. Measurements at these stations, where the approximation of linear trend is more suitable, can compensate for the contribution of the stations in the volcanic area. Thus, in areas affected by volcanic activity the SL projections on the grid can provide more reliable results with respect to the ones obtained by picking up a single GNSS station.

The above results indicate that in the areas of the Mediterranean considered in this study, the VLM contribution from IPCC AR6 on average underestimates the effective VLM resulting in lower or higher future sea levels in zones undergoing active subsidence and uplift. In some areas, such as the Po delta and the Phlegraean fields where VLM rates are particularly high, the differences are extremely large.

Figure 6 shows the maps of the SL at 2100 and 2150 (relative to 2020) for the considered Mediterranean coasts in the most optimistic (SSP1-1.9 and Tlim1.5°) and pessimistic (SSP5-8.5 and

Figure 2. (a) GNSS VLM rate at the grid points. VLM rates on the geographical grid are shown in figure 2 of the supplementary material. (b) GNSS VLM rate at PSMSL stations ordered by increasing longitude. (c) Revised SL at 2100 (relative to 2020) in the SSP5-8.5 scenario at the grid points and (d) at PSMSL stations. (e) Difference between revised and IPCC AR6 SL at 2100 at the grid points and (f) at PSMSL stations. (The correspondence between grid point index and latitude-longitude, PSMSL station index and the station name are shown in tables 1 and 2 of the supplementary material).

Tlim 5°) scenarios. Areas undergoing high rates of land subsidence result in a SL up to 2.9 m at 2150 (relative to 2020) in the worst scenarios. These regions correspond to low lying coastal zones such as river deltas, lagoons, reclamation areas (e.g. the Po delta in Italy, the Thessaloniki plain in Greece and the Rhone delta in France, among others) and volcanic zones (e.g. the Aeolian archipelago and Pantelleria Island in Southern Italy). Conversely, the areas of the Galilee coast (Israel) and the Phlegrean fields (Italy), show a slower sea level rise due to land uplift in response to tectonics and volcanism that characterize these areas. Due to the high uplift rate, in the most optimistic scenarios, both the Galilee coast and Phlegrean fields area show a SL variation at

2150 (relative to 2020) of about 0.5 and −0.7 m, respectively.

The SL projections are more reliable in coastal areas characterized by continuous deformations mainly induced by steady tectonic processes, such as Po, Ebro, and Rhône deltas, Chalastra plain and the coast of Israel. On the other hand, for regions characterized by intense volcanic activity, such as the Aegean Sea around Santorini, Ikaria, and Rhodes islands (Greece), the linear approximation for the VLM can be less precise due to the time variability of the deformation. In this respect, the Aeolian islands represent an exception since they are characterized by a generalized and linear subsidence due to the peculiar activity of the volcanic arc.
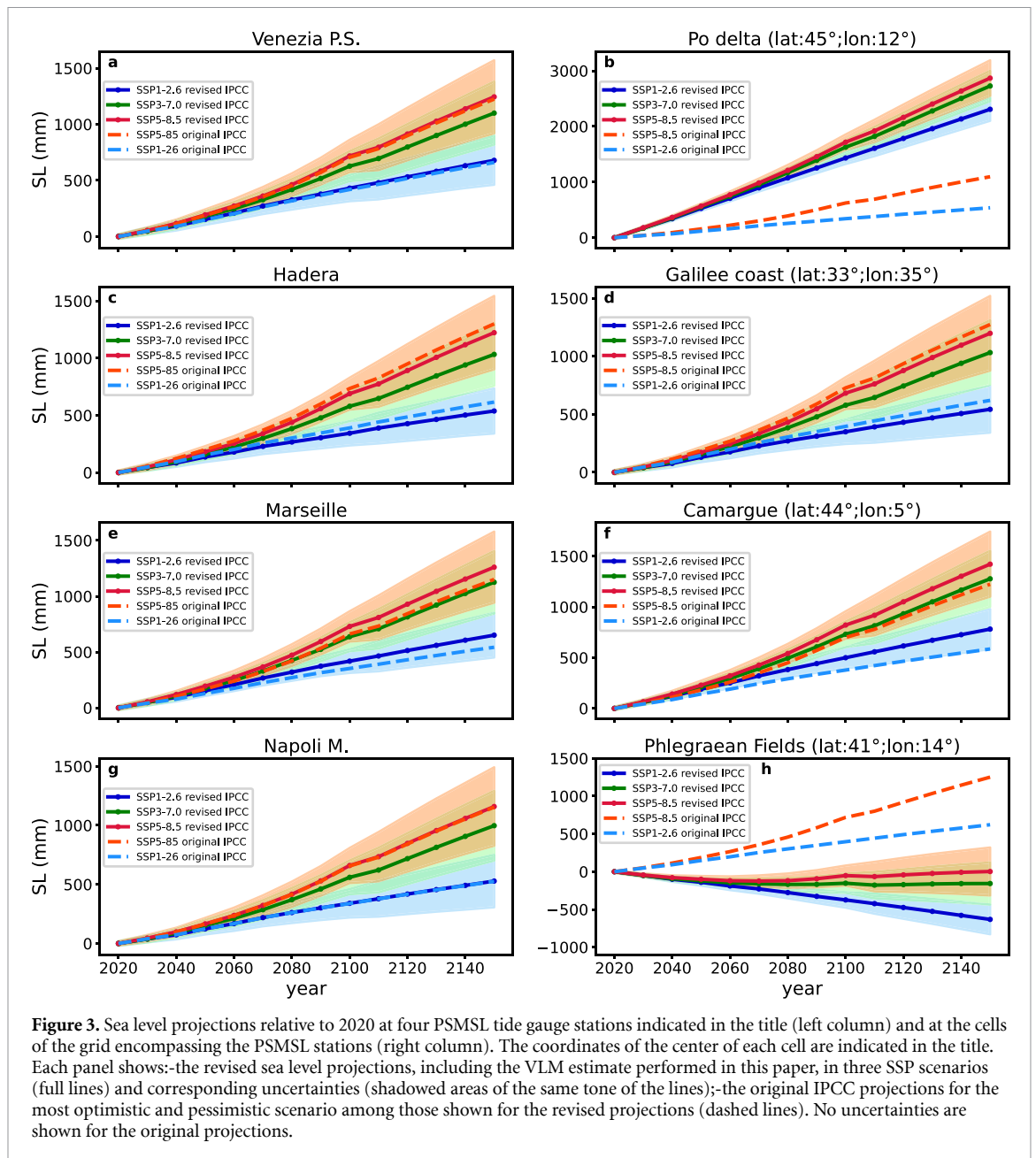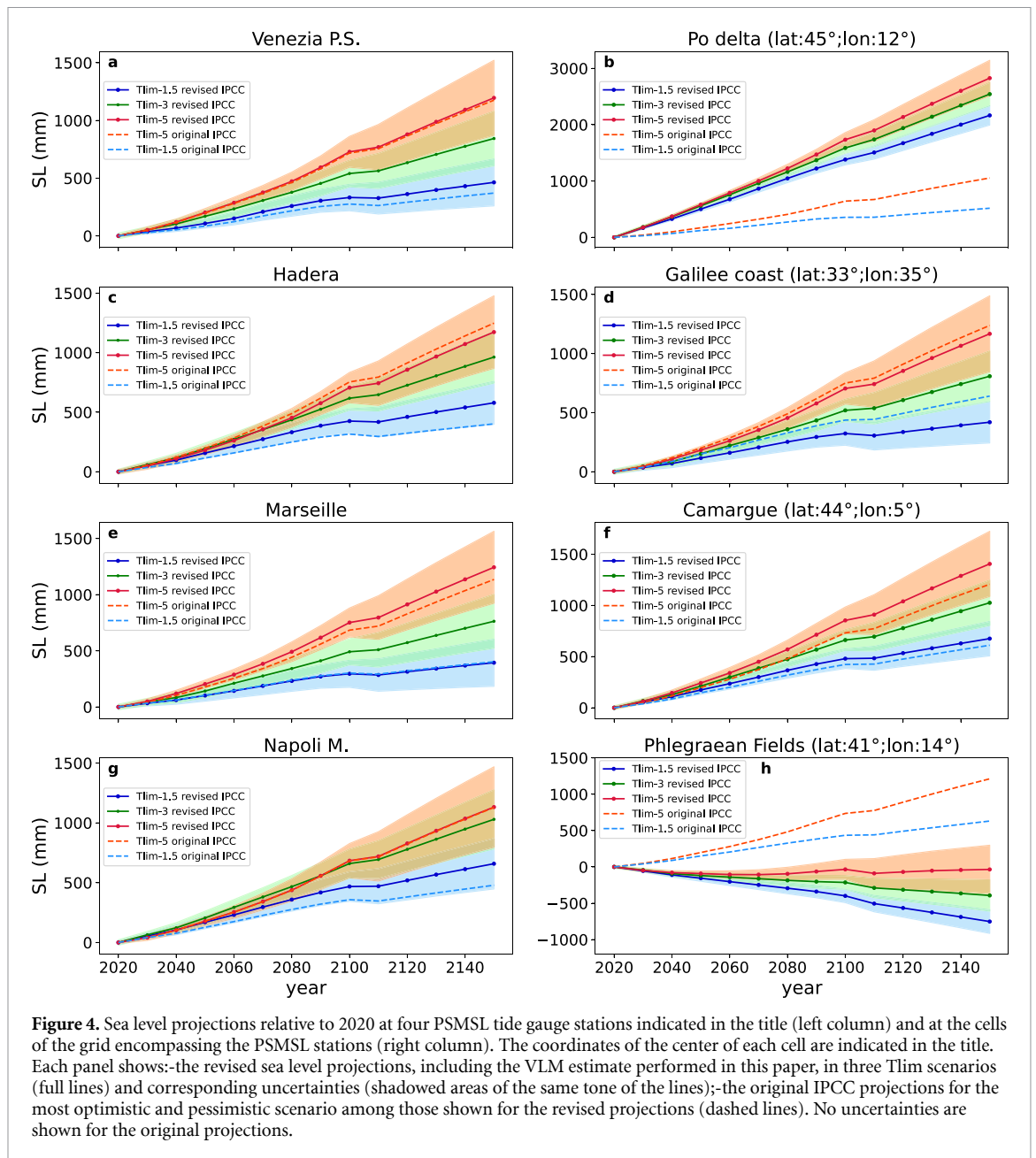
Figure 3. Sea level projections relative to 2020 at four PSMSL tide gauge stations indicated in the title (left column) and at the cells of the grid encompassing the PSMSL stations (right column). The coordinates of the center of each cell are indicated in the title. Each panel shows:-the revised sea level projections, including the VLM estimate performed in this paper, in three SSP scenarios (full lines) and corresponding uncertainties (shadowed areas of the same tone of the lines);-the original IPCC projections for the most optimistic and pessimistic scenario among those shown for the revised projections (dashed lines). No uncertainties are shown for the original projections.

Along the coasts of Turkey, part of Slovenia and Croatia and in North Africa, the lack of available geodetic data (except for Alexandria-Egypt and some stations in Morocco) prevents the calculation of revised SL projections in these areas. Previous studies, based on geological and geo-archaeological observations along the coasts of North Africa (Anzidei *et al* 2011a, Bouaziz *et al* 2003, Benjamin *et al* 2017 and references therein), indicate that this area is characterized by an overall vertical tectonic stability in the last 125 ka BP and especially during the late Holocene, implying that significant deviations from the SL projections

estimated by the IPCC by 2100–2150 are not expected. Conversely, similar studies along the southwest coasts of Turkey, have shown the relevant role of tectonic land subsidence in the flooding of coastal zones (Lambeck 1995, Anzidei *et al* 2011b, Kızıldağ *et al* 2023).

5.1. Exposed zones
By combining the SL projections with the available topographic elevation, it is possible to identify the coastal zones of the Mediterranean most exposed to flooding in the next decades. These correspond to
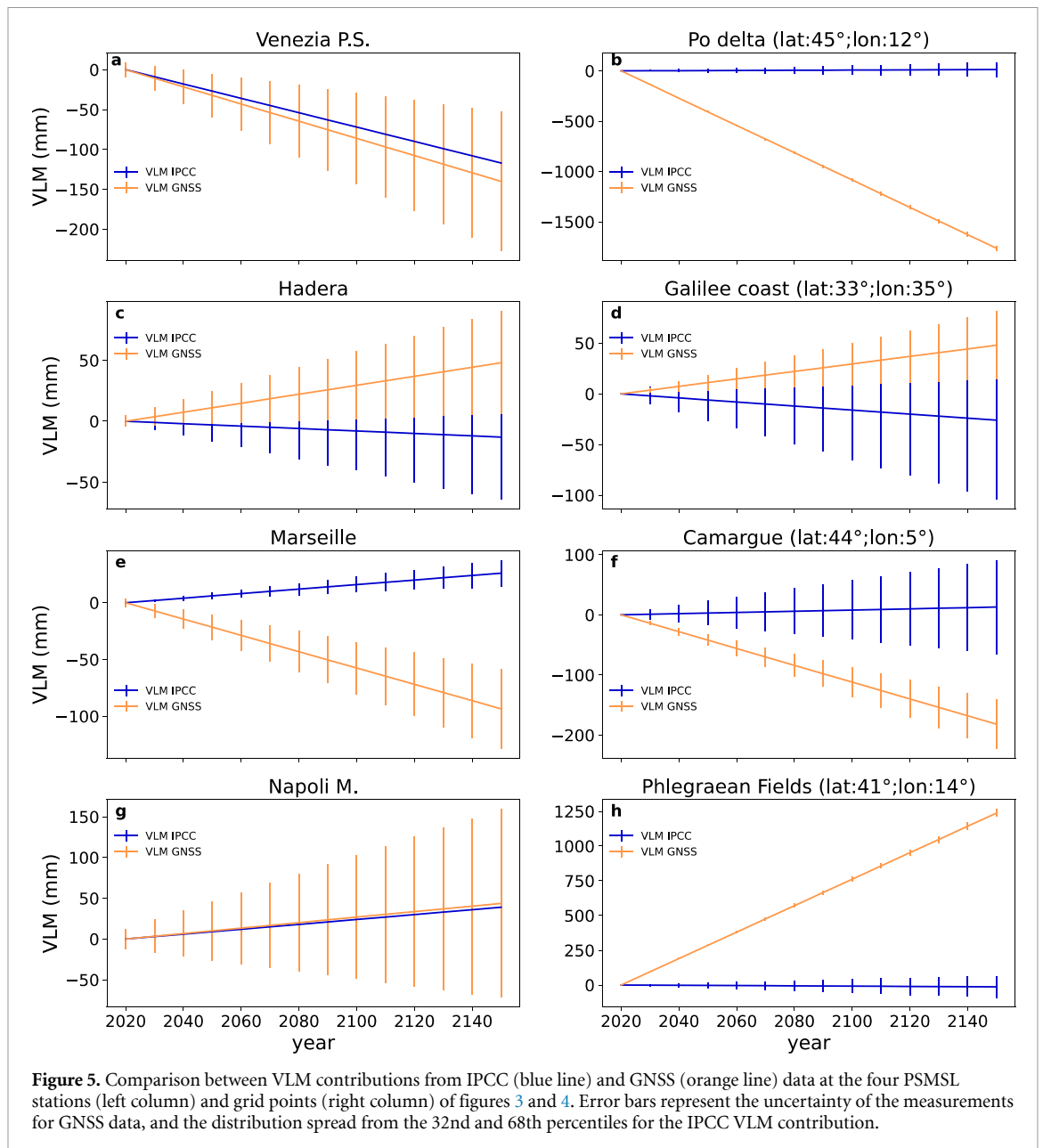
Figure 4. Sea level projections relative to 2020 at four PSMSL tide gauge stations indicated in the title (left column) and at the cells of the grid encompassing the PSMSL stations (right column). The coordinates of the center of each cell are indicated in the title. Each panel shows:-the revised sea level projections, including the VLM estimate performed in this paper, in three Tlim scenarios (full lines) and corresponding uncertainties (shadowed areas of the same tone of the lines);-the original IPCC projections for the most optimistic and pessimistic scenario among those shown for the revised projections (dashed lines). No uncertainties are shown for the original projections.

low elevated areas where the exposure to flooding increases the lower is their elevation above the mean sea level. By making use of the geoprocessing facilities provided by GIS and the availability of datasets of territorial data from EUDEM (a combination of SRTM and ASTER GDEM for the European part and SRTM only for the North-African part from Morocco to Egypt and the Levant for Cyprus, Israel, and Lebanon, https://asterweb.jpl.nasa.gov/gdem.asp), the lowest elevation coastal zones of the Mediterranean region have been identified. The territorial analysis considered about 44.000 km of Mediterranean coastlines, including islands. The analysis of EUDEM data involved the selection of three

coastal altimetric classes above the sea level for the three intervals $[-3, 0]$, $[0, 1]$ and $[1, 2]$ m. Each selected area was then identified on high-resolution satellite images of Digital Globe (Digital Globe Quickbird, which is roughly 65 cm pan-sharpened), to check the morphological correspondence with the altimetric analysis. The analysis identified 163 main coastal plains distributed in 15 countries facing the Mediterranean coasts (figure 7) that correspond to an area of about 38.529 km² and a coastal length of about 7613 km (table 5 of the supplementary material). For these areas the flooding is often favored by lack of natural barriers (e.g. dune belts) and gentle sloping coastal morphology ($<10\%$). Several of these

Figure 5. Comparison between VLM contributions from IPCC (blue line) and GNSS (orange line) data at the four PSMSL stations (left column) and grid points (right column) of figures 3 and 4. Error bars represent the uncertainty of the measurements for GNSS data, and the distribution spread from the 32nd and 68th percentiles for the IPCC VLM contribution.
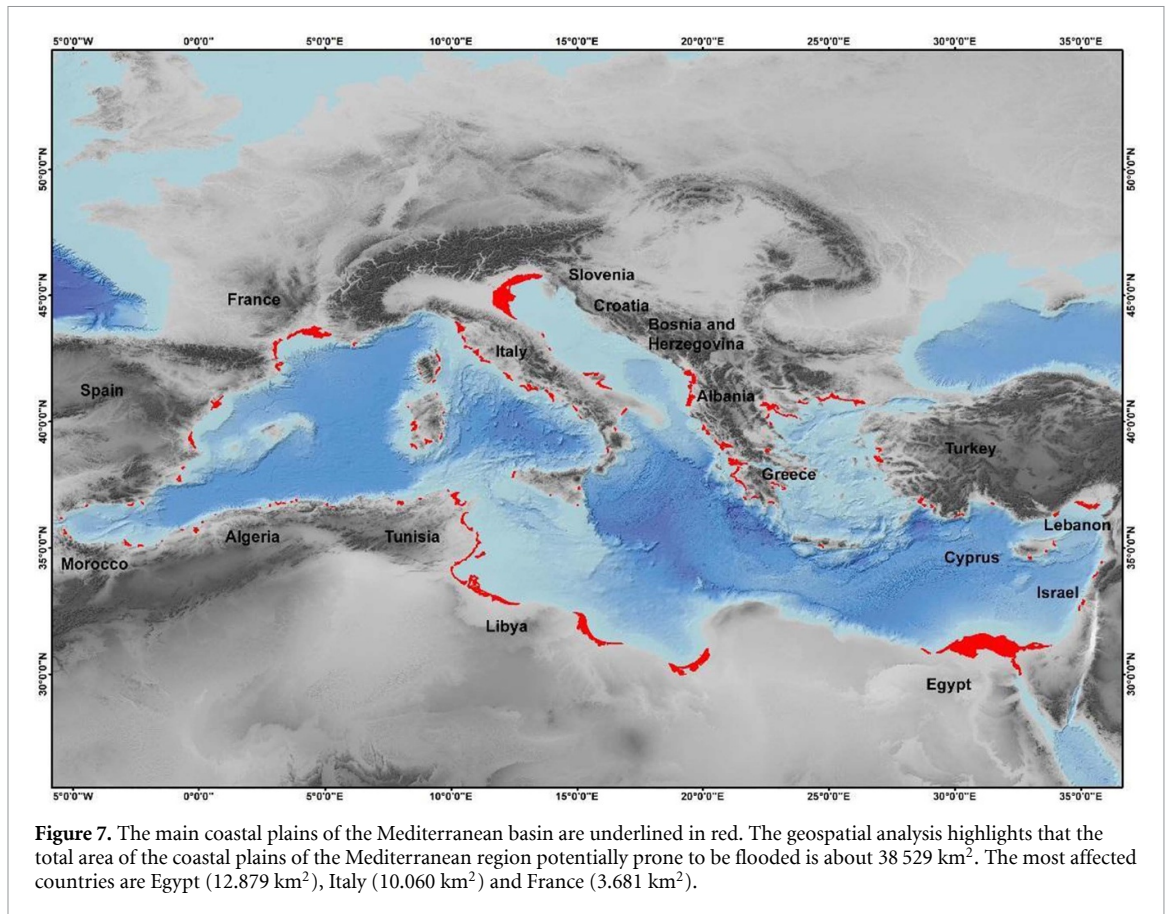
areas are affected by land subsidence, coastal erosion and anthropogenic pressure that accelerate the flooding process, exposing them to increasingly coastal hazard in the next decades, including heritage sites (Reimann *et al* 2018). The most exposed are those of Egypt (12.879 km^2), Italy (10.060 km^2) and France (3.681 km^2). In these countries, the river deltas of Nile (Egypt, about 12.879 km^2), Po (Italy, about 4.000 km^2) and Rhone (France, about 2.000 km^2), which are undergoing high rates of land subsidence due to natural (soil compaction) and anthropogenic (ground fluid exploitation) processes (Syvitski *et al* 2009, Bohannon 2010, Cenni *et al* 2021, Pont *et al* 2002), are at high risk of flooding in 2050–2100–2150,

as shown by the revised SL projections show in figure 6 It is worth noting that most of the population living along the coasts of the Mediterranean is not aware of SL rise, land subsidence and related coastal hazard that impact on the environment, coastal infrastructures, and human activities (Loizidou *et al* 2023). In addition, the current resident population in the Mediterranean countries is about 450 million with a possible rise to 700 million by 2100. The higher population density is found in large coastal cities as well as thousands of small villages placed even below 2 m above the sea level which are highly exposed to SL rise (Papathanassiou and Gabrielides 1999).
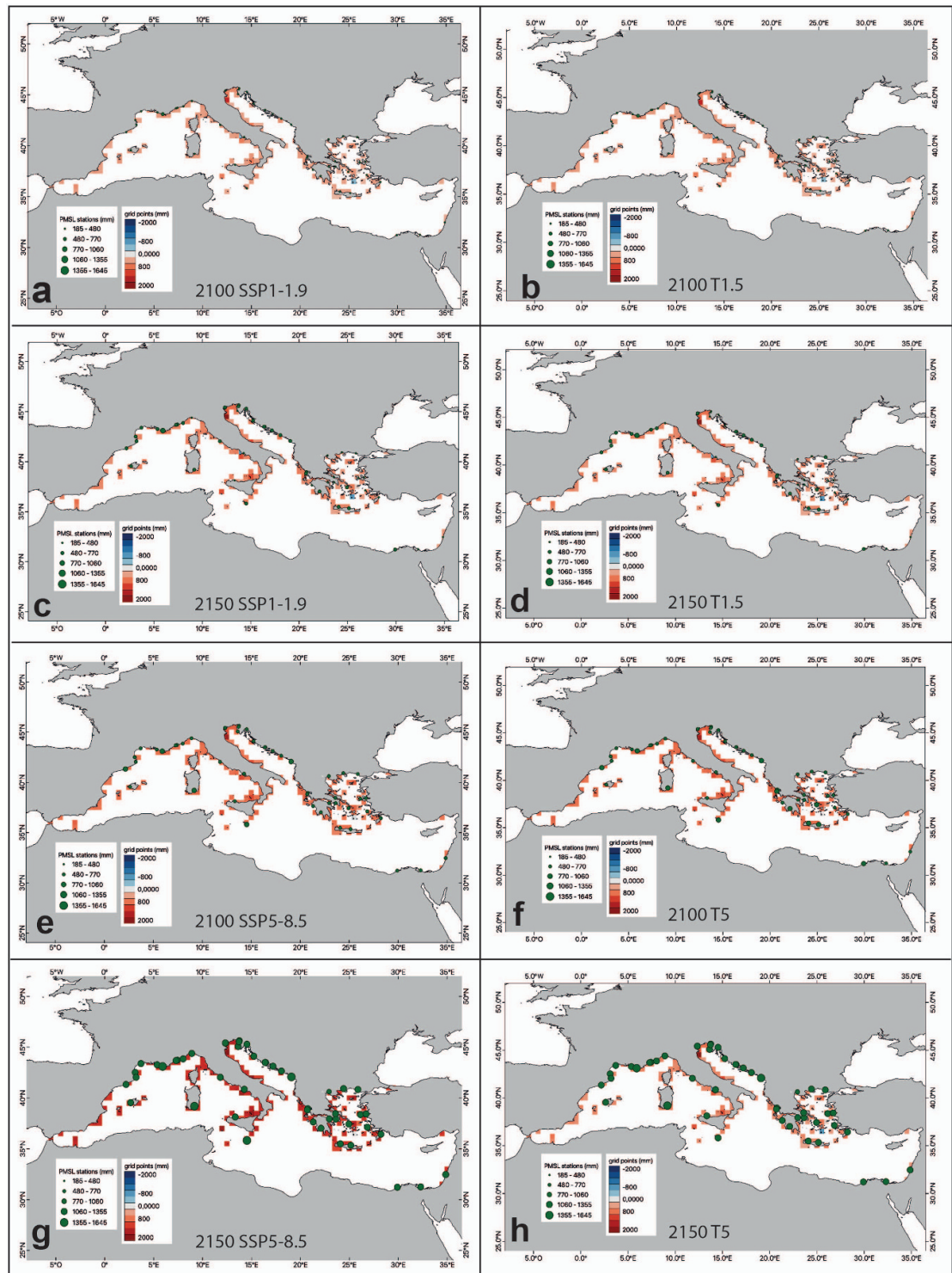
Figure 6. Sea level projections at 2100 (left column) and 2150 (right column) relative to 2020, for SSP and Tlim scenarios at the PSMSL tide gauges (green dots) and on a geographical grid of 0.5° × 0.5° in the Mediterranean Sea (color scale). The maps are obtained by combining the IPCC AR6 projections at regional scales with the VLM derived from GNSS data. Only grid points that include GNSS stations are represented. The VLM in each cell is obtained by calculating the median of all the GNSS measurements contained in the given cell. Panel (a)/(b): RCP1-1.9 2100/2150; panel (c)/(d): Tlim 1.5 °C 2100/2150; panel (e)/(f): RCP5-8.5 2100/2150; panel (c)/(d): Tlim 5 °C 2100/2150.

Figure 7. The main coastal plains of the Mediterranean basin are underlined in red. The geospatial analysis highlights that the total area of the coastal plains of the Mediterranean region potentially prone to be flooded is about 38 529 km^2. The most affected countries are Egypt (12.879 km^2), Italy (10.060 km^2) and France (3.681 km^2).

6. Conclusions

In this study we showed that VLM can significantly increase the future sea levels along the coasts of the Mediterranean basin. The results of the analysis, which includes geodetic rates of VLM in the SL projections, indicate that the new estimates of SL show significant deviations, up to the 62%, from the IPCC AR6 projections.

This implies that in the following years, about 19.000 km of low-lying coastal plains of the Mediterranean will be increasingly exposed to marine flooding and coastal hazard. The effects of the VLM are particularly relevant in river deltas and lagoons and in the unstable volcanic areas, such as the Aeolian islands and Aegean Sea. A large portion of the coast of Italy, Greece, Spain, and France is subsiding thus accelerating the SL rise. The coast of Israel is slightly uplifting and the VLM will locally counterbalance the SL rise. A similar behavior is observed in the volcanic area of the Phlegrean fields (Italy), which is currently uplifting at a high rate of about 9.5 mm yr^{-1}, posing critical conditions for the local coastal infrastructures and human activities. The lack of available public geodetic data for the coasts of Turkey, part of Slovenia, Croatia and North Africa prevented the calculation of revised SL projections. For these areas further analysis is needed to assess the current trend of VLM since the

SL rise will in any case have consequences on the low elevated coasts.

The revised SL projections for the Mediterranean discussed in this letter can support adaptation options for coastal planning for multiple case scenarios of SL rise. Moreover, the information provided in this study can be relevant to mitigate the risk of damaging flooding, which will be increasingly common in case of storm surges and the eventual tsunamis. Finally, the revised SL projections suggest the need to improve science-based dissemination about the impacts of the SL rise toward the coastal populations of the Mediterranean to raise their awareness on this global threat.

Data availability statement

- The sea level projections associated with the Intergovernmental Panel on Climate Change Sixth Assessment Report are available at the following link: https://zenodo.org/record/6382554.
- The sea level projections developed in this work are available at the website www.savemedcoasts2.eu/index.php/en/results. The VLM rates on the geographical grid are available at the same link.
- The VLM rates at the selected PSMSL stations are available in table 2 of the supplementary material.

Acknowledgments

References

Altamimi Z, Collilieux X and Métivier L 2011 Itrf2008: an improved solution of the international terrestrial reference frame *J. Geod.* **85** 457–73

Antonioli F *et al* 2017 Sea-level rise and potential drowning of the Italian coastal plains: flooding risk scenarios for 2100 *Quat. Sci. Rev.* **158** 29–43

Anzidei M *et al* 2017 Flooding scenarios due to land subsidence and sea-level rise: a case study for Lipari Island (Italy) *Terra Nova* **29** 44–51

Anzidei M *et al* 2021 Relative sea-level rise scenario for 2100 along the Coast of South Eastern Sicily (Italy) by InSAR data, satellite images and high-resolution topography *Remote Sens.* **13** 1108

Anzidei M, Antonioli F, Benini A, Lambeck K, Sivan D, Serpelloni E and Stocchi P 2011b Sea level change and vertical land movements since the last two millennia along the coasts of southwestern Turkey and Israel *Quat. Int.* **232** 13–20

Anzidei M, Antonioli F, Lambeck K, Benini A and Soussi M 2011a New insights on the relative sea level change during Holocene along the coasts of Tunisia and western Libya from archaeological and geomorphological markers *Quat. Int.* **232** 5–12

Anzidei M, Doumaz F, Vecchio A, Serpelloni E, Pizzimenti L, Civico R, Greco M, Martino G and Enei F 2020 Sea level rise scenario for 2100 A.D. in the heritage site of pyrgi (Santa Severa, Italy) *J. Mar. Sci. Eng.* **8** 64

Anzidei M, Lambeck K, Antonioli F, Furlani S, Mastronuzzi G, Serpelloni E and Vannucci G 2014 Coastal structure, sea-level changes and vertical motion of the land in the Mediterranean *Sedimentary Coastal Zones from High to Low Latitudes: Similarities and Differences* (Geological Society of London) (https://doi.org/10.1144/SP388.20)

Benjamin J *et al* 2017 Late quaternary sea-level changes and early human societies in the central and eastern Mediterranean basin: an interdisciplinary review *Quat. Int.* **449** 29–57

Bird P, Kagan Y Y, Jackson D D, Schoenberg F P and Werner M J 2009 Linear and nonlinear relations between relative plate velocity and seismicity *Bull. Seismol.* **99** 30973113

Bohannon J 2010 The nile delta's sinking future *Science* **327** 1444–7

Bos M S, Fernandes R M S, Williams S D P and Bastos L 2013 Fast error analysis of continuous GNSS observations with missing data *J. Geod.* **87** 351–60

Bouaziz S, Jedoui Y, Barrier E and Angelier J 2003 Neotectonique affectant les dépots marins tyrrhéniens du littoral sud-est tunisien: implications pour les variations du niveau marin *C.R. Geosci.* **335** 247–54

Bucx T H M, van Ruiten C J M, Erkens G and de Lange G 2015 An integrated assessment framework for land subsidence in delta cities *Proc. IAHS* **372** 485–91

Cenni N, Fiaschi S and Fabris M 2021 Monitoring of land subsidence in the Po River delta (Northern Italy) using geodetic networks *Remote Sens.* **13** 1488

Church J A and White N J 2011 Sea-level rise from the late 19th to the early 21st century *Surv. Geophys.* **32** 585–602

DeConto R M *et al* 2021 The Paris Climate Agreement and future sea-level rise from Antarctica *Nature* **593** 83–89

Devoti R *et al* 2017 Combined velocity field of the Mediterranean region *Ann. Geophys.* **60** 2

Dewey J F, Pitman W C, Ryan W B F and Bonnin J 1973 Plate tectonics and the evolution of the Alpine system *Geol. Soc. Am. Bull.* **84** 3137–80

DISS Working Group 2021 Database of Individual Seismogenic Sources (DISS), version 3.3.0: a compilation of potential sources for earthquakes larger than M 5.5 in Italy and surrounding areas (Istituto Nazionale di Geofisica e Vulcanologia (INGV)) (https://doi.org/10.13127/diss3.3.0)

Esposito A, Pietrantonio G, Bruno V, Anzidei M, Bonforte A, Guglielmino F, Mattia M, Puglisi G, Sepe V and Serpelloni E 2015 Eighteen years of GPS surveys in the Aeolian Islands (southern Italy): open data archive and velocity field *Ann. Geophys.* **58** S0439

Faccenna C *et al* 2014 Mantle dynamics in the Mediterranean *Rev. Geophys.* **52** 283–332

Fenoglio-Marc L, Mariotti A, Sannino G, Meyssignac B, Carillo A, Struglia M and Rixen M 2013 Decadal variability of net water flux at the Mediterranean Sea Gibraltar strait *Glob. Planet. Change* **100** 1–10

Fenoglio-Marc L, Rietbroek R, Grayek S, Becker M, Kusche J and Stanev E 2012 Water mass variation in the Mediterranean and black Seas *J. Geod.* **59–60** 168–82

Ferranti L, Antonioli F, Anzidei M, Monaco C and Stocchi P 2010 The timescale and spatial extent of vertical tectonic motions in Italy: insights from relative sea level changes studies *J. Virtual Exp.* **36** 23

Fox-Kemper B *et al* 2021 Ocean, Cryosphere and Sea Level Change in Climate Change 2021: The Physical Science Basis. Contribution of Working Group I to the Sixth Assessment Report of the Intergovernmental Panel on Climate Change (Cambridge University Press) pp 1211–362

Garner G G *et al* 2021 IPCC AR6 sea-level rise projections Version 20210809 (Accessed 23 June 2023) (https://doi.org/ 10.5281/zenodo.5914709)

Kopp R E *et al* 2023 The framework for assessing changes to sea-level (FACTS) v1.0-rc: a platform for characterizing parametric and structural uncertainty in future global, relative, and extreme sea-level change *EGUsphere [preprint]* (https://doi.org/10.5194/egusphere-2023-14)

Herring T, King R W and McClusky S 2010 GAMIT reference manual, release 10.4. cambridge (MA Massachussetts Institute of Technology)

Higgins S A 2016 Advances in delta-subsidence research using satellite methods *Hydrogeol. J.* **24** 587–600

Horton B P, Khan N S, Cahill N, Lee J S H, Shaw T A, Garner A J, Kemp A C, Engelhart S E and Rahmstorf S 2020 Estimating global mean sea-level rise and its uncertainties by 2100 and 2300 from an expert survey *npj Clim. Atmos. Sci.* **3** 18

Jackson J and McKenzie D 1988 The relationship between plate motions and seismic moment tensors, and the rates of active deformation in the Mediterranean and Middle East *Geophys. J. Int.* **93** 45–73

Jevrejeva S, Williams J, Vousdoukas M I and Jackson L P 2023 Future sea level rise is driving the worst case for extreme sea levels along the global coastline by 2100 *Environ. Res. Lett.* **18** 024037

Jolivet L and Faccenna C 2000 Mediterranean extension and the Africa-Eurasia collision *Tectonics* **19** 1095–106

Kato T 1983 Secular and earthquake-related vertical crustal movements in Japan as deduced from tidal records (1951–1981) *Tectonophysics* **97** 183–200

Kemp A C, Horton B P, Donnelly J P, Mann M E, Vermeer M and Rahmstorf S 2011 Climate related sea-level variations over the past two millennia *Proc. Natl Acad. Sci.* **108** 11017–22

Keogh M E and Törnqvist T E 2019 Measuring rates of present-day relative sea-level rise in low-elevation coastal zones: a critical evaluation *Ocean Sci.* **15** 61–73

Kızıldağ N, Özdaş H, Held W, Spada G and Melini D 2023 Novel insights into the sea level evolution along the coast of Bozburun Peninsula (Turkey): a study on submerged Bronze Age harbor in Çamçalık *Geoarchaeology* **38** 127–260

Kopp R E, Horton R M, Little C M, Mitrovica J X, Oppenheimer M, Rasmussen D J and Tebaldi C 2014 Probabilistic 21st and 22nd century sealevel projections at a global network of tide-gauge sites *Earth's Future* **2** 383–406

Kulp S A and Strauss B H 2019 New elevation data triple estimates of global vulnerability to sea-level rise and coastal flooding *Nat. Commun.* **10** 4844

Lambeck K 1995 Late Pleistocene and Holocene sea-level change in Greece and south-western Turkey: a separation of eustatic, isostatic and tectonic contributions *Geophys. J. Int.* **122** 1022–44

Lambeck K, Antonioli F, Anzidei M, Ferranti L, Leoni G, Scicchitano G and Silenzi S 2011 Sea level change along the italian coast during the Holocene and projections for the future *Quat. Int.* **232** 250–7

Lambeck K and Purcell A 2005 Sea-level change in the Mediterranean Sea since the lgm: model predictions for tectonically stable areas *Quat. Sci. Rev.* **24** 1969–88

Lambeck K, Woodroffe C D, Antonioli F, Anzidei M, Gehrels W R, Laborel J and Wright A J 2010 Paleoenvironmental records, geo physical modeling, and reconstruction of sea-level trends and variability on centennial and longer timescales *Understanding Sea-Level Rise and Variability* (Wiley) pp 61–121

Le Pichon X, Bergerat F and Roulet M J 1988 Plate kinematics and tectonics leading to the Alpine belt formation; A new analysis *Processes in Continental Lithospheric Deformation* vol 218, ed S P Clark, J B C Burchfiel and J Suppe (Geol. Am. Spec. Publ.) pp 111–31

Loizidou X I, Orthodoxou L, Loizides D I, Petsa D and Anzidei M 2023 Adapting to sea level rise: participatory, solution-oriented policy tools in vulnerable Mediterranean areas *Environ. Syst. Decis.* 1–19

Marino C, Ferranti L, Natale J, Anzidei M, Benini A and Sacchi M 2022 Quantitative reconstruction of Holocene ground displacements in the offshore part of the campi flegrei caldera (southern Italy): perspectives from seismo-stratigraphic and archaeological data *Mar. Geol.* **447** 106797

Masson C, Mazzotti S, Vernant P and Doerflinger E 2019 Extracting small deformation beyond individual station precision from dense global navigation satellite system (GNSS) networks in France and Western Europe *Solid Earth* **10** 1905–20

Meli M, Camargo C M L, Olivieri M, Slangen A B A and Romagnoli C 2023 Sea-level trend variability in the Mediterranean during the 1993–2019 period *Front. Mar. Sci.* **10** 1150488

Minderhoud P S J, Erkens G, Pham V H, Bui V T, Erban L, Kooi H and Stouthamer E 2017 Impacts of 25 years of groundwater extraction on subsidence in the Mekong delta Vietnam *Environ. Res. Lett.* **12** 064006

Nguyen H N, Vernant P, Mazzotti S, Khazaradze G and Asensio E 2016 3D GPS velocity field and its implications on the present-day post-orogenic deformation of the Western Alps and Pyrenees *Solid Earth* **7** 1349–63

Nienhuis J H, Kim W, Milne G A, Quock M, Slangen A B A and Törnqvist T E 2023 River deltas and sea-level rise *Annu. Rev. Earth Planet. Sci.* **51** 79–104

Oppenheimer M *et al* 2019 Sea level rise and implications for low-lying islands, coasts and communities *IPCC Special Report on the Ocean and Cryosphere in a Changing Climate* ed H-O Pörtner *et al* (Cambridge University Press) 321–445

Palin R M, Santosh M, Cao W, Li S-S, Hernández-Uribe D and Parsons A 2020 Secular change and the onset of plate tectonics on Earth *Earth Sci. Rev.* **207** 103172

Palmer M D, Domingues C M, Slangen A B A and Boeira Dias F 2021 An ensemble approach to quantify global mean sea-level rise over the 20th century from tide gauge reconstructions *Environ. Res. Lett.* **16** 044043

Papathanassiou E and Gabrielides G P 1999 *State and Pressures of the Marine and Coastal Mediterranean Environment* vol 5, ed G Izzo and S Moretti pp 1–137 (Environmental issues series) (available at: www.eea.europa.eu)

Peltier W R 2001 Chapter 4 Global glacial isostatic adjustment and modern instrumental records of relative sea level history *Int. Geophys.* **75** 65–95

Pont D, Day J W, Hensel P, Franquet E, Torre F, Rioual P, Ibànez C and Coulet E 2002 Response scenarios for the deltaic plain of the Rhône in the face of an acceleration in the rate of sea-level rise with special attention to Salicornia-type environments *Estuaries* **25** 337–58

Rebai S, Philip H and Taboada A 1992 Modern tectonic stress field in the Mediterranean region: evidence for variation in stress directions at different scale *Geophys. J. Int.* **110** 106–40

Reimann L, Vafeidis A T, Brown S, Hinkel J and Tol R S J 2018 Mediterranean UNESCO World Heritage at risk from coastal flooding and erosion due to sea-level rise *Nat. Commun.* **9** 4161

Rizzo A, Vandelli V, Gauci C, Buhagiar G, Micallef A S and Soldati M 2022 Potential sea level rise inundation in the Mediterranean: from susceptibility assessment to risk scenarios for Policy Action *Water* **14** 416

Santamaría-Gómez A, Bouin M-N, Collilieux X and Wöppelmann G 2011 Correlated errors in GPS position time series: implications for velocity estimates *J. Geophys. Res.* **116** B01405

Santamaría-Gómez A and Mémin A 2015 Geodetic secular velocity errors due to interannual surface loading deformation *Geophys. J. Int.* **202** 763–7

Scardino G *et al* 2022 The impact of future sea-level rise on low-lying subsiding coasts: a case study of Tavoliere Delle Puglie (Southern Italy) *Remote Sens.* **14** 4936

Scardino G, Sabatier F, Scicchitano G, Piscitelli A, Milella M, Vecchio A, Anzidei M and Mastronuzzi G 2020 Sea-level rise and shoreline changes along an open sandy coast: case study of Gulf of Taranto, Italy *Water* **12** 1414

Serpelloni E *et al* 2022 Surface velocities and strain-rates in the Euro-Mediterranean region: from massive GPS data processing *Front. Earth Sci.* **10** 907897

Serpelloni E, Vannucci G, Pondrelli S, Argnani A, Casula G, Anzidei M, Baldi P and Gasperini P 2007 Kinematics of the Western Africa-Eurasia plate boundary from focal mechanisms and GPS data *Geophys. J. Int.* **169** 1180–200

Spada G 2017 Glacial Isostatic Adjustment and contemporary sea level rise: an overview *Integrative Study of the Mean Sea Level and Its Components (Space Sciences Series of ISSI* vol 58) ed A Cazenave, N Champollion, F Paul and J Benveniste (Springer)

Strauss B H, Kulp S A, Rasmussen D J and Levermann A 2021 Unprecedented threats to cities from multi-century sea level rise *Environ. Res. Lett.* **16** 11

Strauss B, Tebaldi C, Kulp S, Cutter S, Emrich C, Rizza D and Yawitz D 2014 New York and the surging sea: a vulnerability

assessment with projections for sea level rise and coastal flood risk *Climate Central Research Report* pp 1–42 (available at: https://sealevel.climatecentral.org/uploads/ssrf/NY-Report.pdf)

Syvitski J *et al* 2009 Sinking deltas due to human activities *Nat. Geosci.* **2** 681–6

Tay C *et al* 2022 Sea-level rise from land subsidence in major coastal cities *Nat. Sustain.* **5** 1049–57

Tsimplis M N, Calafat F M, Marcos M, Jordă G, Gomis D, Fenoglio-Marc L and Chambers D 2013 The effect of the NAO on sea level and on mass changes in the Mediterranean Sea *J. Geophys. Res.* **118** 944–52

Vannucci G and Gasperini P 2004 The new release of the database of earthquake mechanisms of the Mediterranean area (EMMA Version 2) *Ann. Geophys.* **47** 307–34

Vecchio A, Anzidei M, Serpelloni E and Florindo F 2019 Natural variability and vertical land motion contributions in the Mediterranean Sea-level records over the last two centuries and projections for 2100 *Water* **11** 1480

Vermeer M and Rahmstorf S 2009 From the cover: global Sea level linked to global temperature *Proc. Natl Acad. Sci.* **106** 21527–32

Vousdoukas M I, Mentaschi L, Voukouvalas E, Verlaan M, Jevrejeva S, Jackson L P and Feyen L 2018 Global probabilistic projections of extreme sea levels show intensification of coastal flood hazard *Nat. Commun.* **9** 2360

Wöppelmann G and Marcos M 2012 Coastal sea level rise in southern Europe and the non-climate contribution of vertical land motion *J. Geophys. Res.* **117** C01007